Available online at www.sciencedirect.com

ScienceDirect

journal homepage: www.JournalofSurgicalResearch.com

Effects of Cross-Clamping on Vascular Mechanics: Comparing Waveform Analysis With a Numerical Model

María Teresa Politi, MD,[a,b,1,*] *Jeanne Ventre, MSc,*[c,1] *Juan Manuel Fernández, MD, PhD,*[a,b] *Arthur Ghigo, PhD,*[d] *Julien Gaudric, MD,*[c,e] *Ricardo Armentano, PhD,*[f] *Claudia Capurro, PhD,*[a,b] *and Pierre-Yves Lagrée, PhD*[a,c]

[a] *Departamento de Ciencias Fisiológicas, Universidad de Buenos Aires, Facultad de Medicina, Laboratorio de Biomembranas, Buenos Aires, Argentina*

[b] *CONICET-Universidad de Buenos Aires, Instituto de Fisiología y Biofísica Bernardo Houssay, Buenos Aires, Argentina*

[c] *Sorbonne Université, Institut Jean Le Rond d'Alembert, CNRS, Paris, France*

[d] *Université de Toulouse, Institut de Mécanique des Fluides de Toulouse (IMFT). CNRS, INPT, UPS, Toulouse, France*

[e] *Hôpitaux Universitaires La Pitié-Salpêtrière, Service de Chirurgie Vasculaire, Paris, France*

[f] *Departamento de Ingeniería Mecánica, Universidad de Buenos Aires, Facultad de Ingeniería, Buenos Aires, Argentina*

ARTICLE INFO

Article history:
Received 22 February 2019
Received in revised form
30 July 2019
Accepted 15 August 2019
Available online xxx

Keywords:
Vascular surgical procedures
Abdominal aorta
Vascular resistance
Compliance
Cardiovascular models

ABSTRACT

Background: Immediate changes in vascular mechanics during aortic cross-clamping remain widely unknown. By using a numerical model of the arterial network, vascular compliance and resistance can be estimated and the time constant of pressure waves can be calculated and compared with results from the classic arterial waveform analysis.

Methods: Experimental data were registered from continuous invasive radial artery pressure measurements from 11 patients undergoing vascular surgery. A stable set of beats were chosen immediately before and after each clamping event. Through the arterial waveform analysis, the time constant was calculated for each individual beat and for a mean beat of each condition as to compare with numerical simulations. Overall proportional changes in resistance and compliance during clamping and unclamping were calculated using the numerical model.

Results: Arterial waveform analysis of individual beats indicated a significant 10% median reduction in the time constant after clamping, and a significant 17% median increase in the time constant after unclamping. There was a positive correlation between waveform analysis and numerical values of the time constant, which was moderate ($\rho = 0.51$; $P = 0.01486$) during clamping and strong ($\rho = 0.77$; $P \leq 0.0001$) during unclamping. After clamping, there was a significant 16% increase in the mean resistance and a significant 23%

* *Corresponding author*. Laboratorio de Biomembranas, Departamento de Ciencias Fisiológicas, Facultad de Medicina, Universidad de Buenos Aires, Paraguay, 2155, C1121 ABG, Buenos Aires, Argentina. Tel.: +54 11-5285-3314; fax: +54 11-38-80-56-40.
E-mail address: mpoliti@fmed.uba.ar (M.T. Politi).

[1] Both authors contributed equally.

https://doi.org/10.1016/j.jss.2019.08.009

decrease in the mean compliance. After unclamping, there was a significant 19% decrease in the mean resistance and a significant 56% increase in the mean compliance.
Conclusions: There are significant hemodynamic changes in vascular compliance and resistance during aortic clamping and unclamping. Numerical computer models can add information on the mechanisms of injury due to aortic clamping.

Introduction

Aortic cross-clamping is a common strategy during cardiovascular surgeries and is essential to some procedures. Yearly, it is performed in over a quarter of a million patients worldwide.[1] However, there is clinical evidence that suggests that the duration of aortic cross-clamping may be related to postoperative morbidity and mortality.[2,3] Because abdominal aortic repair surgeries carry one of the highest postoperative mortality rates among general elective surgeries,[4] insights on the underlying effects of clamping are important for appropriate patient management during this critical surgery phase. Several mechanisms of injury during aortic cross-clamping have been reported, such as myocardial ischemia,[5,6] ischemia-reperfusion injury of the lower limbs, and the gastrointestinal tract[7] and systemic inflammatory response syndrome.[8,9] Recently, attention has been drawn toward the role of vascular compliance in the risk of rupture of abdominal aneurysms,[10,11] the choice of the aortic graft,[12] and the association with postoperative complications of abdominal aneurysm repair.[13,14] However, immediate changes in vascular mechanics during clamping and unclamping interventions are not well established.

Arterial waveform analysis is commonly used to calculate the time constant of the diastolic portion of pressure waves.[15-17] However, this method is unable to estimate by itself the relative contribution of compliance (C) or resistance (R) to the time constant (τ) (i.e., considering $\tau = RC$). By using a numerical model of the arterial network, these important vascular features, compliance, and resistance can be estimated along with the time constant.[18,19] Such a numerical model would therefore offer an appropriate mean of comparison with classic waveform analysis, by comparing the estimated time constants, while offering valuable information on vascular mechanical properties.

We designed an observational study to validate a numerical model of the arterial network against arterial waveform analysis and to evaluate the immediate changes in vascular mechanics after aortic cross-clamping and unclamping during vascular surgeries in adult patients.

Methods

Study design and patient population

This is a cross-sectional, observational, and analytical study evaluating the effect of arterial clamping and unclamping of the abdominal aorta during vascular surgeries. The impact of these interventions on arterial vascular parameters was estimated through the time constant of the diastolic portion of invasive radial arterial pressure tracings during each clamping condition. Patients were evaluated before and after each clamping/unclamping intervention. This study enrolled adult patients undergoing peripheral vascular surgery involving abdominal aortic clamping at the *Hôpital Universitaire Pitié-Salpêtrière* in Paris, France. Exclusion criteria were having (1) an irregular heart rhythm, (2) waveform diastolic values that do not fit a single exponential decay, or (3) a reduced left ventricular ejection fraction (<45%) measured by echocardiography or cardiac magnetic resonance during routine preoperative workup.

Invasive radial artery pressure measurements

Experimental information on arterial pressure changes during vascular surgeries was obtained from continuous invasive radial artery pressure tracings of adult patients undergoing peripheral vascular surgery involving abdominal aortic clamping, as described before.[20,21] Briefly, a fluid-filled catheter from the right radial artery was connected to a disposable pressure transducer (TruWave, Edwards Lifesciences), allowing data registry using an analog-digital converter with internal hardware filters (low-pass frequency set at 20 kHz, high-pass frequency set at 0.05 Hz, MP150, BIOPAC Systems Inc). The AcqKnowledge software was used to record arterial pressure tracings, interpolating data to a final rate of 1000 Hz.

Arterial waveform analysis

Pressure tracings were analyzed using a custom algorithm developed in MATLAB (R2018b, The MathWorks, Inc, Natick, Massachusetts). A stable set of beats from invasive arterial pressure tracings were chosen throughout 20- to 40-s intervals immediately before and after each intervention. Data from the brief transition period (5-30 s) after each clamping/unclamping event were not considered. The beginning of each individual beat was automatically identified using local minimum pressure values. To obtain a mean beat, given physiological variations in the heart rate, the length of each pressure tracing was normalized to the median length of all pressure tracings in that interval using 1-D interpolation. The mean beat was then obtained by averaging the pressure values at each time point.

Because two-element Windkessel models show a single exponential decay during capacitor discharge, we used this feature to automatically detect the onset of the diastole for every cycle (Fig. 1). Starting from the end of the beat (iteration number 0), we evaluated the exponential growth coefficient ($1/\tau$) by sequentially fitting 100-millisecond intervals with 1-millisecond backward steps. The maximum rate of change ($\delta(1/\tau)$) of this coefficient was defined as the onset of the diastole (red triangle, Fig. 1). Finally, pressure data from the

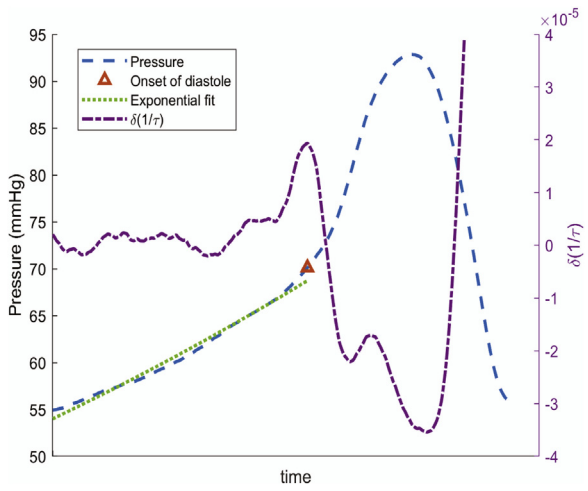

Fig. 1 – Arterial waveform analysis. The x-axis (time) is inverted as to represent the analysis sequence. Starting from the end of the beat (left side of the figure), the exponential growth coefficient (1/τ) of the arterial pressure curve (dashed, blue) was estimated by fitting 100-millisecond intervals with 1-millisecond backward steps. The onset of diastole (red triangle) was obtained from the local maximum of δ(1/τ) (dash-point, purple). Pressure data from the diastolic time interval were fitted to a single exponential function (dots, green) to obtain the final time constant (τ). (Color version of figure is available online.)

entire diastolic period was fitted to a single exponential function to obtain the final diastolic time constant (green dotted line, Fig. 1). The time constant of the diastolic portion of arterial pressure tracings was computed for both individual beats and for the mean beat of each interval for each patient under each condition.

Numerical model

Zero-dimensional (0D) models are the very first level of modeling. These types of models are analogies of electrical circuits, in which pressure stands for voltage and flow rate stands for current, and both quantities are linked through a time-varying ordinary differential equation. The circuit is made up of an assembly of resistors and capacitors that have a physical role: resistors represent the effect of viscous dissipation, whereas capacitors model the compliant effects of arteries. The most widely used model for simulating blood flow is known as the Windkessel model,[22] which was originally composed of only two elements, a resistor (R_2) and a capacitor (C), being able to approximately predict the exponential decay of arterial blood pressure during the diastole right after the aortic valve closes (Fig. 2). This model was further improved by adding another resistor (R_1). The time constant (τ) can be calculated from these parameters considering $\tau = R_2C$.

The general governing equation of the two-element Windkessel model that represents the systemic arterial circuit is the following time-varying ordinary differential equation:

$$p + R_2C\frac{dp}{dt} = (R_1 + R_2)Q + R_1R_2C\frac{dQ}{dt} \quad (1)$$

Equation (1) can be discretized with a forward Euler scheme, where the blood pressure in the systemic vascular circuit (P) is the unknown variable.

$$p^n + R_2C\frac{p^{n+1} - p^n}{\Delta t} = (R_1 + R_2)Q^n + R_1R_2C\frac{Q^{n+1} - Q^n}{\Delta t} \quad (2)$$

The unknown variable of Equation (2) is presented as p^{n+1} (i.e., the blood pressure at time t^{n+1}) and p^n (i.e., the blood pressure at time t^n before t^{n+1}), with $\Delta t = t^{n+1} - t^n$ being the time step. Because pressure $P(t)$ is the unknown variable in Equation (1), the inlet flow rate ($Q(t)$) (i.e., the flow of blood ejected by the left ventricle into the systemic arterial circuit) needs to be imposed. The flow rates Q^n and Q^{n+1} correspond to the inlet flow imposed at times t^n and t^{n+1}, respectively. To mimic a beating heart, a common simplified strategy to model the inlet flow rate is to use half a sine signal.[19] As shown in Figure 2A, an inlet flow rate ($Q(t)$) such as this can be described by two parameters: the amplitude of the inlet flow rate (Q_0) and the ejection time (T_{ej}). The ejection time (T_{ej}) is defined as the percentage of the overall duration of a heart period (T) in

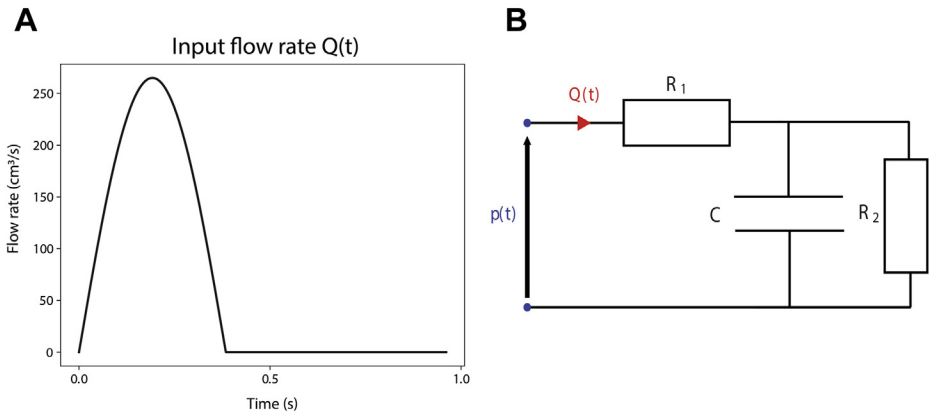

Fig. 2 – Zero-dimensional Windkessel model with three components (two resistors and one capacitor) that accounts for the systemic arterial network. (A) The inlet flow rate (Q(t)) depends on the amplitude of the flow rate (Q_0) and on the ejection time (T_{ej}). (B) Electrical analogy of the Windkessel model, where R_1 and R_2 together represent the total resistance and C represents the capacitance. (Color version of figure is available online.)

which the left ventricle is ejecting blood into the systemic vessels. The heart period (T) is fixed by experimental data. Therefore, the inlet flow rate ($Q(t)$) can be defined by the following expression:

$$\begin{cases} Q(t) = Q_0 \sin\left(\frac{\pi}{T_{ej}} \frac{t}{T}\right) \text{if } 0 < t < T_{ej}T \\ Q(t) = 0 \qquad\qquad \text{if } T_{ej}T \leq t < T, \end{cases} \tag{3}$$

where Q_0 is the amplitude of the sine, T is the heart period ,and T_{ej} is the ejection time. The stroke volume (i.e., the volume ejected by the left ventricle during each heart beat) is defined as the integral of the inlet flow rate ($Q(t)$) over one heart period (T).

The objective of this analysis was to estimate the values of the model parameters R_1, R_2, and C and T_{ej} from each patient for preclamp, postclamp, preunclamp, and postunclamp settings. We defined the vector $\vec{p}$ as the set of parameters (R_1;R_2;C;T_{ej}). By using an inverse method based on experimental blood pressure data, we were able to study how these systemic vascular parameters are affected by the action of aortic clamping. The cost function J measures the error between the results of our model, which depend on $\vec{p}$, and continuous experimental pressure data. This cost function is defined as follows:

$$J(\vec{p}, t) = \left(\int_0^T \left(P_{exp}(t) - P_{num}(\vec{p}, t)^2 dt \right) \right)^{1/2} \tag{4}$$

where P_{exp} is the continuous experimental pressure data and P_{num} is the solution of Equation (1), that is, the simulated results from our model.

The amplitude of the inlet flow rate (Q_0) is a parameter that cannot be estimated because it is related to the total value of resistance through Ohm's law. When the capacitor is fully charged, Equation (1) becomes $P = R_{tot}\, Q$, where R_{tot} is the total resistance ($R_{tot} = R_1 + R_2$). The chosen value for the amplitude of the inlet flow rate (Q_0) is such that the stroke volume does not drastically change with aortic clamping. The assumption of keeping a constant stroke volume throughout aortic clamping is based on the fact that all enrolled patients had a preserved left ventricular ejection fraction (≥45%), and on published experimental data.[23-25] Normal values for systolic volume are usually between 70 and 90 mL.

The model parameters were found through the following optimization process: at each iteration, for an initial set of parameters $\vec{p}$, Equation (1) was solved with the forward Euler scheme from Equation (2) generating $P_{num}(\vec{p}, t)$. The cost function $J(\vec{p}, t)$ from Equation (4) was then calculated and aimed to be minimized. The method used to minimize the cost function J was a Basin-Hopping method[26,27] that runs a gradient-based algorithm L-BFGS-B[28] at each iteration. At each step, the algorithm finds a new set of parameters that decrease the value of J so that the value of numerical pressure would be closer to the value of experimental pressure; then, it would move on to the next step. When convergence was finally reached, the optimal patient-dependent set of parameters (R_1;R_2;C;T_{ej}) were found so that numerical pressure would resemble experimental pressure ($P_{num} \simeq P_{exp}$) for preclamp, postclamp, preunclamp, and postunclamp settings.

Ethical issues

The study is in accordance with the ethical principles of the Declaration of Helsinki.[29] The study protocol was assessed by the institutional review board of the Hôpital Universitaire Pitié-Salpêtrière. In accordance with French law, because this is an observational study involving only routine clinical practices and therefore offering minimal risk for patients, the need of an informed consent form was waived. The study is registered with the national French data protection authority (Commission Nationale de l'Informatique et des Libertés) (N° 20190709113900).

Statistical analysis

A one-way analysis was conducted to assess the distribution of each covariate. Continuous variables were summarized using mean and standard deviation for normally distributed variables and median and interquartile range (IQR) for non-normally distributed variables. Categorical variables were summarized with percentages in each category. Group comparisons involved the two-tailed paired t-tests for normally distributed variables, Wilcoxon signed-rank test for non-normally distributed variables, and chi-square or Fischer's exact tests for categorical variables. Normality was assessed formally by Shapiro–Wilk tests. Correlation was assessed with Pearson's correlation coefficient (ρ) for variables with a multivariate normal distribution and with Spearman's correlation coefficient (rs) for variables with a non-normal multivariate distribution. Global agreement was assessed by visual examination of the Bland-Altman plots.[30] Bland-Altman agreement plots represent the difference between two measurements on the y-axis plotted against the average of these measurements on the x-axis. The mean difference between the two measurements is called the center of agreement and is represented by a central horizontal line on the plot. The upper/lower limits of agreement are ±1.96 standard deviation of the mean difference. The gap between the center of agreement and the x-axis (corresponding to zero differences) is called the bias. Normality in the distribution of the differences was verified formally by Shapiro–Wilk tests. Two-tailed tests were considered statistically significant at the 0.05 level. A percentage bias (bias/mean waveform analysis time constant) of 20% or less was considered acceptable. Statistical analysis was performed using R software version 1.0.136[31] (packages ggplot2,[32] BlandAltmanLeh,[33] MVN[34]).

Results

The invasive arterial pressure measurements of 14 patients undergoing vascular surgery were assessed; 3 patients were excluded (2 for having an irregular rhythm and 1 for having waveforms that did not fit a single exponential decay). There were 11 patients included in the final study, of which 9 had an infrarenal abdominal aortic aneurysm and underwent open repair surgery with either an aorto-aortic tube graft (3 patients) or an aorto-bi-iliac graft (6 patients). The remaining 2 patients had occlusive artery disease and underwent aorto-bifemoral bypass surgeries. All selected aortic clamps were

Table 1 – Patient clinical characteristics.

Patient	Age, y	Sex	DB	SMK	HT	DL	Height, m	Weight, kg
1	84	M	N	N	Y	Y	1.65	57
2	84	M	N	Y	Y	Y	1.62	65
3	80	M	N	Y	Y	N	1.70	74
4	46	M	N	Y	Y	Y	1.61	65
5	81	F	N	Y	Y	Y	1.56	48
6	64	M	N	Y	N	Y	1.90	110
7	49	F	N	Y	N	Y	1.67	71
8	58	F	N	Y	N	N	1.59	54
9	67	M	Y	Y	Y	Y	1.82	105
10	65	M	N	Y	Y	Y	1.75	85
11	78	F	N	Y	N	N	1.50	42
Total	69 ± 14	63.0%	9.1%	90.9%	63.6%	72.7%	1.67 ± 0.12	70.5 ± 21.9

Absolute values are presented as mean ± standard deviation (SD).
DB = diabetes mellitus; SMK = smoking status; HT = arterial hypertension. DL = dyslipidemia.

infrarenal. No patients had an aortic repair because of graft or native aortic infection in this series. Most patients with aneurysms and all patients with occlusive disease had arterial calcifications. However, these were mainly restricted to the iliac arteries, without affecting the femoropopliteal region. Patients were mostly elder (69 ± 14 years-old) males (63.6%) with hypertension (63.6%) and dyslipidemia (72.7%) who were current smokers (90.9%). Table 1 shows patients' full clinical characteristics. Table 2 indicates patients' comorbidities and medication.

Changes in the time constant measured by arterial waveform analysis

Experimental data involved continuous radial artery pressure tracings from 11 abdominal aortic clamps and unclamps. The median values of the time constant of the diastolic portion of arterial pressure waves from 20- to 40-s intervals before and after each intervention measured by the arterial waveform analysis were compared. In all individual patients, the median time constant decreased after clamping and increased after unclamping (Supplementary table 1). After abdominal aortic clamping, there was a significant 10% reduction in the overall median time constant of the diastolic portion of arterial pressure waves. Before clamping, the overall median time constant was 2.12 (IQR: 1.54-2.36) seconds, whereas after clamping, it was 1.79 (IQR: 1.48-1.91) seconds; this difference was statistically significant ($P = 0.0033$). After abdominal aortic unclamping, there was a significant 17% increase in the overall median time constant. Before unclamping, the overall median time constant was 1.77 (IQR: 1.52-1.99) seconds, whereas after clamping, it was 1.90 (IQR: 1.73-2.32) seconds; this difference was also statistically significant ($P = 0.0033$).

Table 2 – Patient comorbidities and medication.

Patient	CAD	HF	IC	Aspirin	Statins	BB	ACEI/ARBs	CCB	Diuretics
1	N	N	N	Y	Y	N	N	Y	Y
2	Y	N	Y	Y	Y	Y	Y	N	N
3	Y	N	Y	Y	Y	Y	Y	N	Y
4	N	N	N	Y	Y	N	Y	N	N
5	Y	N	Y	Y	Y	Y	Y	N	Y
6	Y	N	N	Y	Y	Y	Y	N	N
7	N	N	Y	Y	Y	Y	Y	N	Y
8	N	N	Y	Y	Y	N	Y	N	N
9	Y	N	Y	Y	Y	Y	Y	N	Y
10	N	N	N	Y	Y	N	N	Y	N
11	N	N	N	Y	Y	N	Y	N	N
Total	45.5%	0%	54.5%	100%	100%	54.5%	81.8%	18.2%	45.5%

CAD = coronary artery disease; HF = heart failure; IC = intermittent claudication; BB = beta-blockers; ACEI = angiotensin-converting enzyme inhibitors; ARBs = angiotensin II receptor antagonists; CCB = calcium channel blockers.

Comparison between the absolute values of the time constant measured by the arterial waveform analysis and by a numerical model

The time constant of the mean beat of each patient before and after each intervention was calculated using the parameters of the numerical model (Fig. 3). These values were compared to the time constant of the mean beat of each patient before and after each intervention measured by the arterial waveform analysis. Both methods suggested that the time constant decreased after clamping and increased after unclamping (Fig. 4). There was a positive significant correlation between the values of the time constant measured by both methods, which was moderate ($\rho = 0.51$; $P = 0.01486$) during clamping and strong ($\rho = 0.77$; $P \leq 0.0001$) during unclamping (Fig. 5). Bland-Altman plots showed appropriate agreement between the experimental and numerical values of the diastolic time constant. In both settings, the bias was small (13.7% for clamping, 14.7% for unclamping). For nearly all cases, the differences between the two measurements were within the limits of agreement (Table 3). However, there was a possible systematic bias observed for high values of the diastolic time constant during aortic unclamping, where numerical values seemed to overestimate waveform analysis values (Fig. 5).

Comparison between proportional changes in the time constant measured by arterial waveform analysis and by a numerical model

The overall proportional change in the diastolic time constant after each intervention was calculated for each method. Clamping produced a median 10% (IQR: 8%-21%) decrease in the time constant measured by the arterial waveform analysis as compared with a median 16% (IQR: 7%-19%) decrease in the time constant measured by the numerical model; there were no significant differences between these estimations ($P = 0.7646$). Unclamping produced a median 18% (IQR: 9%-21%) increase in the time constant measured by the arterial waveform analysis as compared with a median 21% (IQR: 14%-30%) decrease in the time constant measured by the numerical model; again, there were no significant differences between these estimations ($P = 0.2061$) (Fig. 4).

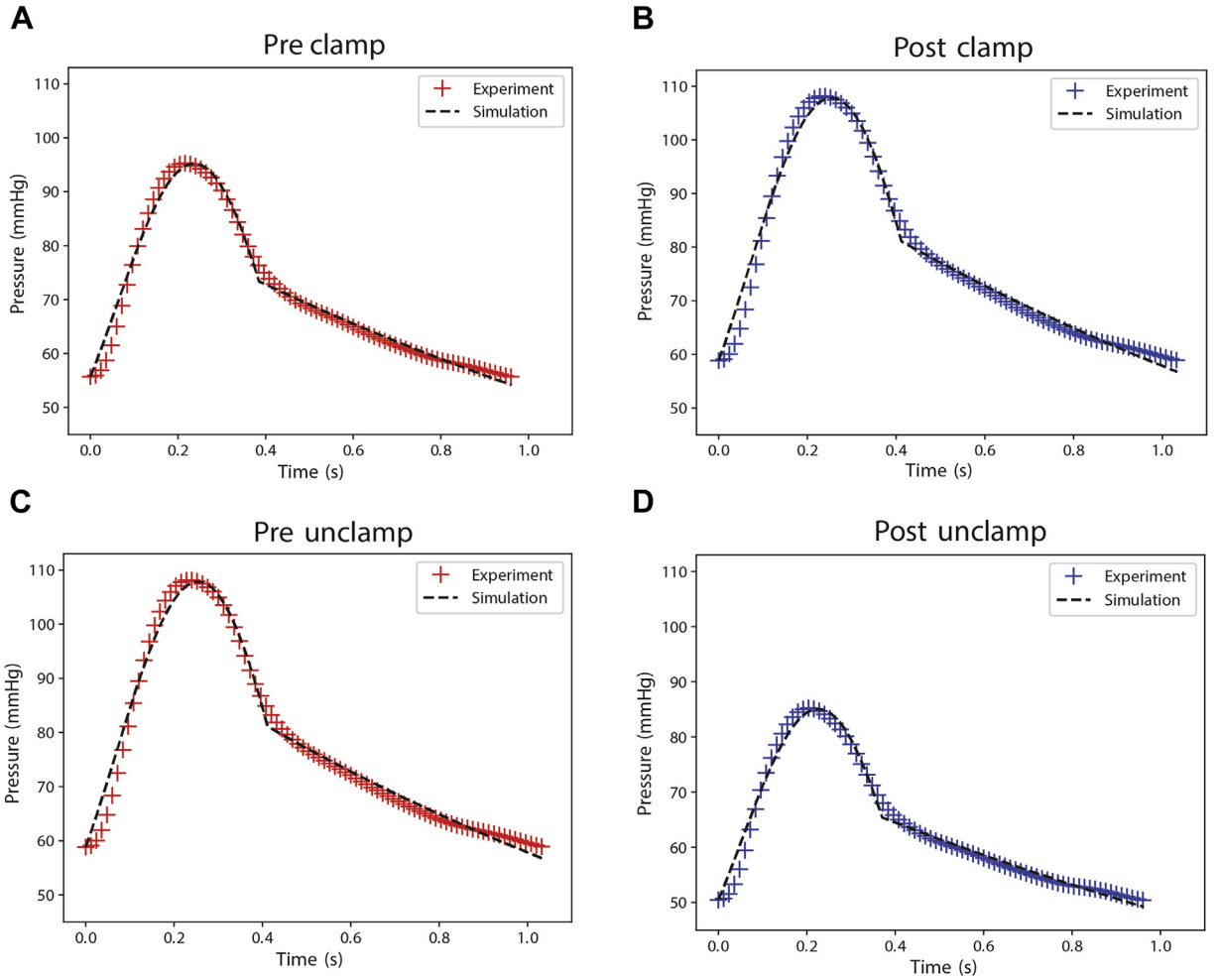

Fig. 3 – Arterial pressure waveform for one representative patient (patient 3) before (A) and after (B) aortic clamping and before (C) and after (D) aortic unclamping during vascular surgery. Colored + symbols indicate experimental values of arterial pressure. Black dashed lines indicate simulated arterial pressure values found solving Equation 1 for the numerical model of the systemic arterial network. (Color version of figure is available online.)

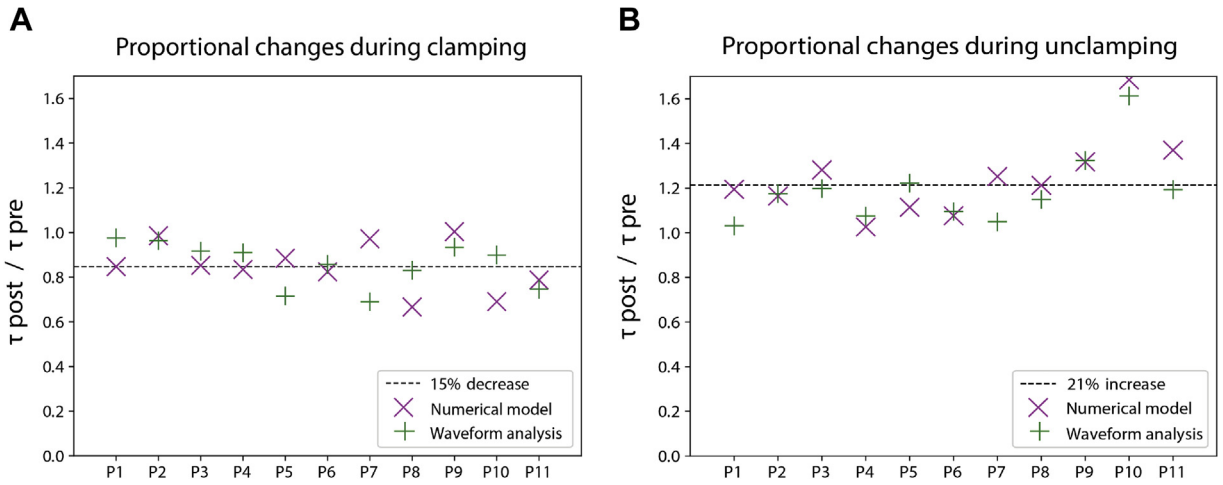

Fig. 4 – Comparison between methods of proportional changes in the diastolic time constant (τ). Changes estimated by a numerical model (× symbols in magenta) and by the arterial waveform analysis (+symbols in green) are expressed as the ratios between postclamp and preclamp (A) and postunclamp and preunclamp (B). Figure inlet indicates the median percentage change for the diastolic time constant (τ) estimated by a numerical model (dashed line). (Color version of figure is available online.)

Overall proportional changes in total vascular resistance and compliance estimated by a numerical model

Because the total resistance ($R_{tot} = R_1+R_2$) and compliance (C) of the systemic arterial circuit are model parameters, their overall proportional changes during clamping and unclamping were calculated (Supplementary table 2). After abdominal aortic clamping, there was a significant 16% increase in the mean total vascular resistance (R_{tot}) (from 1237.1 ± 250.2 dyn s cm^{-5} to 1435.0 ± 317.7 dyn s cm^{-5}; $P = 0.0019$) and a significant 23% decrease in the mean vascular compliance (C) (from 3.0 ± 1.1 mL/mmHg to 2.3 ± 0.9 mL/mmHg; $P = 0.0002$). After abdominal aortic unclamping, there was a significant 19% decrease in mean the total vascular resistance (R_{tot}) (from 1241.9 ± 234.1 dyn s cm^{-5} to 1003.8 ± 221.9 dyn s cm^{-5}; $P = 0.0007$) and a significant 56% increase in the mean vascular compliance (C) (from 2.7 ± 1.0 mL/mmHg to 4.1 ± 1.8 mL/mmHg; $P = 0.001952$) (Fig. 6).

Discussion

This study indicates that immediate changes in vascular mechanics after abdominal aortic clamping and unclamping during vascular surgeries can be estimated by a numerical model.

One of the first important findings in this study is that the diastolic time constant of radial arterial pressure waves before and after aortic cross-clamping and unclamping during vascular surgeries in adult patients can be calculated by two different methods: the arterial waveform analysis and using a mathematical model of the arterial network. Our findings indicate that the absolute values of the diastolic time constant seem to differ in some patients when comparing both methods, thus limiting the value of the numerical model to make patient-specific estimations. Furthermore, there may be a systematic overestimation when applying the numerical model to high values of the diastolic time constant during unclamping. However, the overall correlation and agreement between measurements seem appropriate, and the overall percentage changes in the diastolic time constant estimated by each method show no significant differences. In addition, the subset in which there is a possible systematic bias represents only 9% of all data. These results suggest that although the numerical model may have limitations for making patient-specific predictions, it can identify accurately and with precision the direction and magnitude of proportional changes in the diastolic time constant as compared with arterial waveform analysis. Although other studies have validated the predictions of numerical models with pressure waveform morphology measured experimentally in human subjects, the correspondence between model predictions and actual arterial pressure waves was only qualitatively assessed.[35-37] On the contrary, in our study, the correlation and agreement between methods for measuring the diastolic time constant were systematically assessed and quantified.

The second important finding in our study is that the diastolic time constant decreases 10%-16% during clamping and increases 18%-21% during unclamping. These results comply with the only previous study, to our knowledge, that reported changes in the arterial diastolic time constant during aortic clamping.[38] After abdominal aortic occlusion with a balloon catheter during 2 min in 7 male dogs, Van den Bos *et al.* reported a significant 16.6% decrease in the diastolic time constant of arterial pressure waves.[38] This result is comparable to ours in the location of the aortic clamping, the duration of the clamp, and in the magnitude of the reported change. In our study, the decrease in the diastolic time constant during clamping and its increase during unclamping were systematically found in all patients. In addition, as mentioned previously, there was a good agreement between both methods,

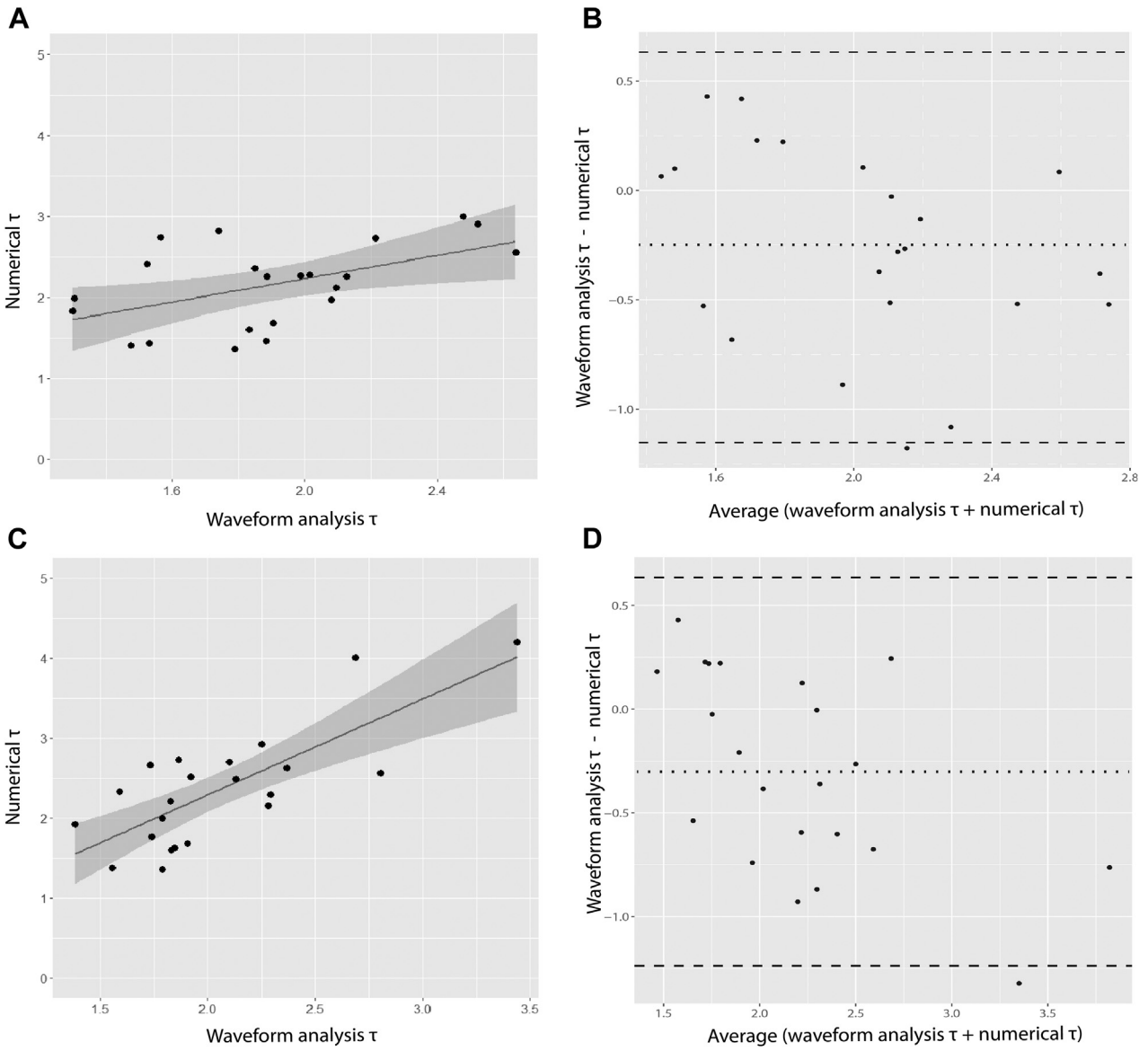

Fig. 5 – Correlation and agreement between methods. Correlation between the absolute values of the diastolic time constant (τ) estimated by a numerical model and by the arterial waveform analysis during clamping (A) and unclamping (C), indicating a moderate ($\rho = 0.51$; $P = 0.01486$) and a strong ($\rho = 0.77$; $P = < 0.0001$) positive correlation, respectively. Bland-Altman agreement plots indicating appropriate agreement between the two methods during aortic clamping (B) and unclamping (D). The dotted line is the mean difference between methods; the dashed lines are the upper and lower limits of agreement (±1.96 SD of the mean difference).

experimental and numerical, regarding the direction and the magnitude of proportional change. These findings allowed us to presume that the numerical model of the arterial network would offer appropriate estimations of the immediate changes in vascular mechanics after aortic clamping and unclamping.

The third important finding in our study is that during abdominal aortic clamping total vascular resistance (R_{tot}) increases and compliance (C) decreases, while the opposite occurs during unclamping. Although we cannot discard the influence of biological regulatory phenomena, a possible explanation for the increase in total vascular resistance (R_{tot}) during clamping is that parallel resistances are being blocked out of the circuit. Likewise, a probable explanation for the decrease in compliance (C) during clamping is that the overall surface of the system gets smaller. During unclamping the opposite events occur, added to a local vasodilation of ischemic areas due to the accumulation of adenosine, lactate, and carbon dioxide during clamping.[8] This phenomenon possibly explains why in our study the percentage changes in vascular resistance, and especially in vascular compliance, are larger after unclamping than after clamping. Our results are in agreement with previous studies on the hemodynamic changes of abdominal aortic clamping.[23-25,33,39] Montenij *et al.*

Table 3 – Agreement results from Bland-Altman plots.

Estimate	Clamping	Unclamping	Units
Bias	−0.260	−0.302	S
95% CI bias	−0.462 to −0.058	−0.514 to −0.090	S
Percentage bias	13.7	14.7	%
Upper LoA	0.632	0.635	S
95% CI upper LoA	0.283 to 0.982	0.268 to 1.002	S
Lower LoA	−1.152	−1.238	S
95% CI lower LoA	−1.502 to −0.803	−1.605 to −0.871	S

Percentage changes are calculated regarding the mean time constant measured by the arterial waveform analysis.
CI = confidence interval; LoA = limits of agreement.

reported that mean vascular resistance increases 16.8% 5 min after abdominal aortic cross-clamping and decreases 36.3% 10 min after clamp release in 22 patients undergoing elective open abdominal aortic aneurysm repair.[23] Attia *et al.* informed a significant 7.1% increase in mean vascular resistance 1-3 min after abdominal aortic cross-clamping in 5 male patients.[39] Biais *et al.* described a significant 44.5% increase in the median total vascular resistance 10 min after abdominal aortic cross-clamping in 24 pigs.[24] Van Den Bos *et al.* informed a 22.7% increase in mean vascular resistance after abdominal aortic occlusion with a balloon catheter during 2 min in 7 male dogs.[38] Martín-Cancho *et al.* went even further to describe the dynamic changes through time in mean total vascular resistance following abdominal aortic clamping and unclamping in 18 pigs undergoing laparotomy.[25] These authors report that mean total vascular resistance increases 38.0% 30 min after clamping and 39.1% 60 min after clamping. They also inform

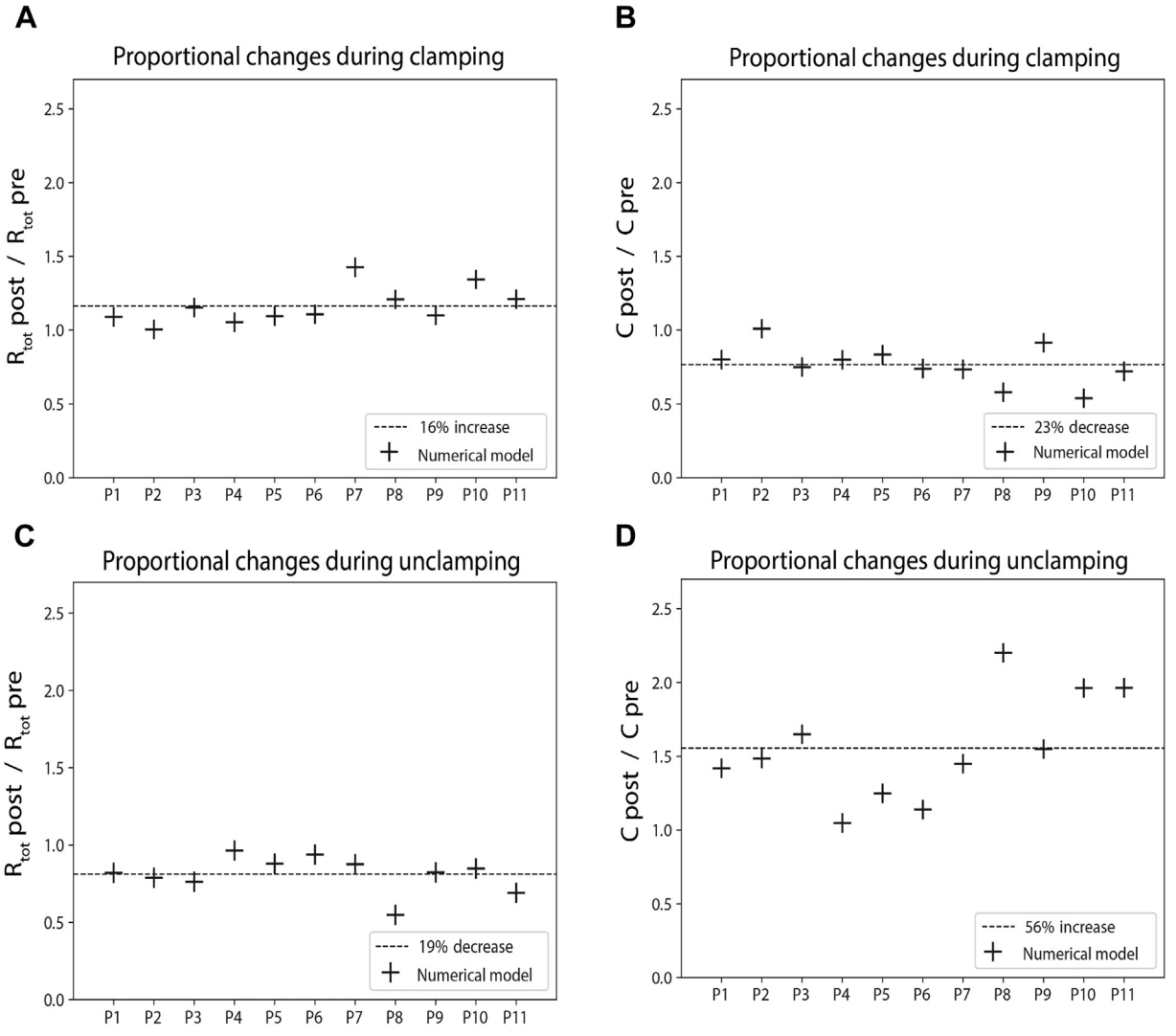

Fig. 6 – Proportional changes in total vascular resistance (R_{tot}) and compliance (C) during clamping and unclamping. Changes are expressed as the ratios between postclamp and preclamp (A and B) and postunclamp and preunclamp (C and D).

changes in mean total vascular resistance following abdominal aortic unclamping: a 55.6% decrease after 5 min, a 42.4% decrease after 30 min, and a 33.2% decrease after 60 min. Globally, these studies report changes 3-60 min after clamping/unclamping events, while our results indicate immediate effects, generally within the first minute after the event. The importance of stressing the time at which data are collected, especially regarding aortic unclamping, is highlighted by the dynamic changes described by Martín-Cancho *et al.*.[25] In addition, although these previous studies report changes in total vascular resistance after clamping/unclamping, most fail to report changes in vascular compliance. Only Attia *et al.* inform a 23.2% decrease in vascular compliance 1-3 min after abdominal aortic cross-clamping in 5 male patients, and Van Den Bos *et al.* inform a 17.1% decrease in vascular compliance after abdominal aortic occlusion with a balloon catheter during 2 min in 7 male dogs.[38,39] Both results are in accordance with the 23% decrease in mean vascular compliance found in our study. To our knowledge, this is the first study to analyze immediate changes in vascular compliance in adult patients after clamping and unclamping using both experimental data and a numerical model of the arterial network.

The strength of this study resides in the availability of experimental data from human subjects in a real-world scenario involving vascular surgeries that are analyzed with appropriate agreement by both arterial waveform analysis and a numerical model. These results open the possibility of exploring the clinical implications of these changes for both patient intraoperative monitoring and vascular prosthesis safety. Numerical estimations of the immediate hemodynamic changes related to aortic clamping and unclamping could help develop clinical predictive models to identify patients at risk of perioperative ischemic injury. In addition, information on the immediate changes in the mechanical properties of the arterial network during vascular surgery could help improve the design of vascular prosthesis and surgical instruments, by guiding the selection of materials and the geometrical configuration of these tools according to the wide range of mechanical changes that may take place. However, some limitations in this study must be acknowledged. First, our results are based on the assumption that stroke volume does not change during clamping and unclamping interventions. This assumption was made on the lack of continuous data on stroke volume throughout the surgery—which is not routine practice during surgical interventions—or of a numerical heart model to simulate this variable during clamping/unclamping interventions. However, because (1) changes in stroke volume reported in the literature during aortic cross-clamping are inconsistent,[40-43] (2) we are interested in studying only the immediate impact of clamping/unclamping, and (3) all patients had a preserved left ventricular ejection fraction (i.e., $\geq$45%), we assume that this is a fair assumption to make. Second, the absolute values of the diastolic time constant found by each method were slightly different for some patients. This could possibly be due to intrinsic differences between these two methods because the numerical estimations arise from fitting the numerical pressure wave to the entire experimental pressure curve, whereas estimations from the arterial waveform analysis are based on an exponential function that is fitted only to the diastolic part of the experimental pressure curve. In addition, numerical estimations use a cost function J that is the square error between the model's estimations and the experimental pressure waveform. The fact that the error is squared conditions the cost function J to penalize more a large local error than it penalizes two small local errors, therefore influencing the final numerical estimation of the time constant. A third important limitation to acknowledge is that the number of subjects considered in this study is small. Because individual patient-specific characteristics, such as comorbidities and medication, could have an influence on our results, a larger clinical study with more patients and enough power to adjust for relevant clinical characteristics would be necessary to increase the external validity of our conclusions.

In all, this study has validated this numerical model of the arterial network, and determined the magnitude of change of both vascular resistance and compliance during aortic clamping/unclamping. The next step would be to design a large prospective cohort study to explore the clinical implications of these immediate changes in vascular mechanics. This future study would require pre-established clinical outcomes and enough statistical power to adjust for covariates and potential confounding. The results of this study could translate to patient care by contributing to the development of perioperative risk models and by guiding the design of vascular prosthesis and surgical instruments.

Conclusion

There are significant hemodynamic changes in vascular compliance and resistance during aortic clamping, which may have clinical implications for both patient intraoperative monitoring and vascular prosthesis safety. Numerical computer models can add information on the mechanisms of injury due to aortic clamping.

Acknowledgment

The authors would like to thank the anesthesiologists and nurses from the vascular surgery ward at the *Hôpital Universitaire Pitié-Salpêtrière*, Dr José María Fullana and Dr Sandra Wray for their help and support in this study, and also Dr Diego Crippa for his clinical advisement.

This work was supported by the 2016 ECOS-SUD grant (project number A16S03) between the Ministerio de Ciencia y Tecnología from Argentina and the Ministère de l'Education Nationale et de la Recherche from France, by the PICT 2015-2168 grant from the Agencia Nacional de Promoción Científica y Tecnológica from Argentina, and by the Universidad de Buenos Aires travel grants from Argentina (number EXP-UBA 32.318/2018).

Supplementary data

Supplementary data to this article can be found online at https://doi.org/10.1016/j.jss.2019.08.009.

Disclosure

The authors have nothing to disclose.

REFERENCES

1. D'Agostino RS, Jacobs JP, Badhwar V, et al. The Society of Thoracic Surgeons adult cardiac surgery database: 2017 update on outcomes and quality. *Ann Thorac Surg*. 2017;103:18–24.
2. Salsano A, Giacobbe DR, Sportelli E, et al. Aortic cross-clamp time and cardiopulmonary bypass time: prognostic implications in patients operated on for infective endocarditis. *Interact Cardiovasc Thorac Surg*. 2018;1:328–335.
3. Ruggieri VG, Bounader K, Verhoye JP, et al. Prognostic impact of prolonged cross-clamp time in coronary artery bypass grafting. *Heart Lung Circ*. 2018;27:1476–1482.
4. Karthikesalingam A, Vidal-Diez A, Holt PJ, et al. Thresholds for abdominal aortic aneurysm repair in England and the United States. *N Engl J Med*. 2016;24:2051–2059.
5. Croal BL, Hillis GS, Gibson PH, et al. Relationship between postoperative cardiac troponin I levels and outcome of cardiac surgery. *Circulation*. 2006;114:1468–1475.
6. Onorati F, De Feo M, Mastroroberto P, et al. Determinants and prognosis of myocardial damage after coronary artery bypass grafting. *Ann Thorac Surg*. 2005;79:837–845.
7. Li C, Li YS, Xu M, et al. Limb remote ischemic preconditioning for intestinal and pulmonary protection during elective open infrarenal abdominal aortic aneurysm repair: a randomized controlled trial. *Anesthesiology*. 2013;118:842–852.
8. Zammert M, Gelman S. The pathophysiology of aortic cross-clamping. *Best Pract Res Clin Anaesthesiol*. 2016;30:257–269.
9. Norwood MGA, Bown MJ, Sayers RD. Ischaemia-reperfusion injury and regional inflammatory responses in abdominal aortic aneurysm repair. *Eur J Vasc Endovasc Surg*. 2004;28:234–245.
10. Wang X, Li X. A fluid–structure interaction-based numerical investigation on the evolution of stress, strength and rupture potential of an abdominal aortic aneurysm. *Comput Methods Biomech Biomed Engin*. 2013;16:1032–1039.
11. van 't Veer M, Buth J, Merkx M, et al. Biomechanical properties of abdominal aortic aneurysms assessed by simultaneously measured pressure and volume changes in humans. *J Vasc Surg*. 2008;48:1401–1407.
12. Gawenda M, Knez P, Winter S, et al. Endotension is influenced by wall compliance in a latex aneurysm model. *Eur J Vasc Endovasc Surg*. 2004;27:45–50.
13. Morris L, Stefanov F, Hynes N, Diethrich EB, Sultan S. An experimental evaluation of device/arterial wall compliance mismatch for four stent-graft devices and a multi-layer flow modulator device for the treatment of abdominal aortic aneurysms. *Eur J Vasc Endovasc Surg*. 2016;51:44–55.
14. Sekhri AR, Lees WR, Adiseshiah M. Measurement of aortic compliance in abdominal aortic aneurysms before and after open and endoluminal repair: preliminary results. *J Endovasc Ther*. 2004;11:472–482.
15. MacKenzie Ross RV, Toshner MR, Soon E, Naeije R, Pepke-Zaba J. Decreased time constant of the pulmonary circulation in chronic thromboembolic pulmonary hypertension. *Am J Physiol Heart Circ Physiol*. 2013;305:H259–H264.
16. Pagnamenta A, Vanderpool R, Brimioulle S, Naeije R. Proximal pulmonary arterial obstruction decreases the time constant of the pulmonary circulation and increases right ventricular afterload. *J Appl Physiol*. 2013;114:1586–1592.
17. Assad TR, Brittain EL, Wells QS, et al. Hemodynamic evidence of vascular remodeling in combined post- and precapillary pulmonary hypertension. *Pulm Circ*. 2016;6:313–321.
18. Ghigo AR, Abou Taam S, Wang X, Lagrée PY, Fullana JM. A one-dimensional arterial network model for bypass graft assessment. *Med Eng Phys*. 2017;43:39–47.
19. Formaggia L, Lamponi D, Tuveri M, Veneziani A. Numerical modeling of 1D arterial networks coupled with a lumped parameters description of the heart. *Comput Methods Biomech Biomed Engin*. 2006;9:273–288.
20. Politi MT, Ghigo A, Fernandez JM, et al. The dicrotic notch analyzed by a numerical model. *Comput Biol Med*. 2016;1:54–64.
21. Politi MT, Wray SA, Fernandez JM, et al. Impact of arterial cross-clamping during vascular surgery on arterial stiffness measured by the augmentation index and fractal dimension of arterial pressure. *Health Technol*. 2016;6:229–237.
22. Westerhof N, Lankhaar JW, Westerhof BE. The arterial Windkessel. *Med Biol Eng Comput*. 2009;47:131–141.
23. Montenij LJ, Buhre WF, De Jong SA, et al. Arterial pressure waveform analysis versus thermodilution cardiac output measurement during open abdominal aortic aneurysm repair: a prospective observational study. *Eur J Anaesthesiol*. 2015;32:13–19.
24. Biais M, Calderon J, Pernot M, et al. Predicting fluid responsiveness during infrarenal aortic cross-clamping in pigs. *J Cardiothorac Vasc Anesth*. 2013;27:1101–1107.
25. Martín-Cancho MF, Crisóstomo V, Soria F, et al. Physiologic responses to infrarenal aortic cross-clamping during laparoscopic or conventional vascular surgery in experimental animal model: comparative study. *Anesthesiol Res Pract*. 2008;2008:581948.
26. Wales DJ, Doye JP. Global optimization by basin-hopping and the lowest energy structures of Lennard-Jones clusters containing up to 110 atoms. *J Phys Chem*. 1997;101:5111–5116.
27. Wales DJ, Scheraga HA. Global optimization of clusters, crystals, and biomolecules. *Science*. 1999;285:1368–1372.
28. Byrd RH, Lu P, Nocedal J, Zhu C. A limited memory algorithm for bound constrained optimization. *SIAM J Scientific Comput*. 1995;16:1190–1208.
29. World Medical Association. World Medical Association Declaration of Helsinki: ethical principles for medical research involving human subjects. *JAMA*. 2013;27:2191–2194.
30. Bland JM, Altman DG. Statistical methods for assessing agreement between two methods of clinical measurement. *Lancet*. 1986;8:307–310.
31. R Core Team. *R: a Language and Environment for statistical computing*. Vienna, Austria: R Foundation for Statistical Computing; 2013.
32. Wickham H. *ggplot2: Elegant Graphics for data analysis*. New York: Springer-Verlag; 2016.
33. Lehnert B. *BlandAltmanLeh: plots (slightly extended) Bland-Altman plots*. 2015. R package version 0.3.1.
34. Korkmaz S, Goksuluk D, Zararsiz G. Mvn: An R package for assessing multivariate normality. *R J*. 2014;6:151–162.
35. Reymond P, Merenda F, Perren F, Rüfenacht D, Stergiopulos N. Validation of a one-dimensional model of the systemic arterial tree. *Am J Physiol Heart Circ Physiol*. 2009;297:H208–H222.
36. Reymond P, Bohraus Y, Perren F, Lazeyras F, Stergiopulos N. Validation of a patient-specific one-dimensional model of the systemic arterial tree. *Am J Physiol Heart Circ Physiol*. 2011;301:H1173–H1182.
37. Mynard JP, Smolich JJ. One-dimensional haemodynamic modeling and wave dynamics in the entire adult circulation. *Ann Biomed Eng*. 2015;43:1443–1460.

38. Van Den Bos GC, Westerhof N, Elzinga G, Sipkema P. Reflection in the systemic arterial system: effects of aortic and carotid occlusion. *Cardiovasc Res*. 1976;10:565–573.
39. Attia RR, Murphy JD, Snider M, Lappas DG, Darling RC, Lowenstein E. Myocardial ischemia due to infrarenal aortic cross-clamping during aortic surgery in patients with severe coronary artery disease. *Circulation*. 1976;53:961–965.
40. Stokland O, Molaug M, Thorvaldson J, Ilebekk A, Kiil F. Cardiac effects of splanchnic and non-splanchnic blood volume redistribution during aortic occlusions in dogs. *Acta Physiol Scand*. 1981;113:139–146.
41. Kotake Y, Yamada T, Nagata H, Takeda J, Shimizu H. Descending aortic blood flow during aortic cross-clamp indicates postoperative splanchnic perfusion and gastrointestinal function in patients undergoing aortic reconstruction. *Br J Anaesth*. 2012;108:936–942.
42. Lafanechère A, Albaladejo P, Raux M, et al. Cardiac output measurement during infrarenal aortic surgery: echo-esophageal Doppler versus thermodilution catheter. *J Cardiothorac Vasc Anesth*. 2006;20:26–30.
43. Klotz KF, Klingsiek S, Singer M, et al. Continuous measurement of cardiac output during aortic cross-clamping by the oesophageal Doppler monitor ODM 1. *Br J Anaesth*. 1995;74:655–660.